

On the Reconstructed Fermi Surface in the Underdoped Cuprates

H.-B. Yang,¹ J. D. Rameau,¹ Z.-H. Pan,¹ G. D. Gu,¹ P. D. Johnson,¹

H. Claus,² D. G. Hinks,² and T. E. Kidd³

(1) *Condensed Matter Physics and Materials Science Department,
Brookhaven National Laboratory, Upton, New York 11973, USA*

(2) *Materials Science Division, Argonne National Laboratory, Argonne, Illinois 60439, USA*

(3) *Physics Department, University of Northern Iowa, Cedar Falls, Iowa 50614, USA*

The Fermi surface topologies of underdoped samples of the high- T_c superconductor Bi2212 have been measured with angle resolved photoemission. By examining thermally excited states above the Fermi level, we show that the observed Fermi surfaces in the pseudogap phase are actually components of fully enclosed hole pockets. The spectral weight of these pockets is vanishingly small at the anti-ferromagnetic zone boundary, which creates the illusion of Fermi “arcs” in standard photoemission measurements. The area of the pockets as measured in this study is consistent with the doping level, and hence carrier density, of the samples measured. Furthermore, the shape and area of the pockets is well reproduced by phenomenological models of the pseudogap phase as a spin liquid.

Understanding the pseudogap regime in the high T_c superconducting cuprates is thought to be the key to understanding the high T_c phenomenon in general [1]. An important component of that understanding will be the determination of the nature of the low lying normal state electronic excitations that evolve into the superconducting state. It is therefore critically important to know the exact nature of the Fermi surface (FS) associated with these materials. Photoemission studies of the pseudogap regime reveal gaps in the spectral function in directions corresponding to the copper-oxygen bonds and a FS that seemingly consists of disconnected arcs falling on the surface defined within the framework of a weakly interacting Fermi liquid [2]. A number of different theories have attempted to explain these phenomena in terms of competing orders whereby the full FS undergoes a reconstruction reflecting the competition [3, 4]. An alternative approach recognizes that the superconducting cuprates evolve with doping from a Mott insulating state with no low energy charge excitations to a new state exhibiting properties characteristic of both insulators and strongly correlated metals.

Several theories have been proposed to describe the cuprates from the latter perspective [5–7]. One such approach is represented by the so-called YRZ ansatz [6], which, based on the doped RVB spin liquid concept [8], has been shown to successfully explain a range of experimental observations in the underdoped regime [9–12]. The model is characterized by two phenomena, a pseudogap that differs in origin from the superconducting gap and hole-pockets that satisfy the Luttinger sum rule for a Fermi surface defined by both the poles and zeros of the Green’s function at the chemical potential [13]. The pockets manifest themselves along part of the FS as an “arc” possessing finite spectral weight corresponding to the poles of the Green’s function as in a conventional metal. The remaining “ghost” component of the Fermi surface is defined by the zeros of the Green’s function and therefore possesses no spectral weight to be directly observed. Importantly, the zeros of the Green’s function at

the chemical potential coincide with the magnetic zone boundary associated with the underlying antiferromagnetic order of the Mott insulating state and therefore restrict the pockets to lying on only one side of this line. The model further predicts that the arc and ghost portions of the FS are smoothly connected to pockets. Several theoretical studies indicate that within this framework the pockets have an area that scales with the doping [6, 10]. Recent photoemission studies have indeed provided some indication that the pseudogap regime is characterized by hole pockets centered in the nodal direction [14, 15]. In the present study, we demonstrate for the first time that the FS of the underdoped cuprates in the normal state is characterized by hole pockets with an area proportional to the doping level and a Fermiology as described above. These measurements, well fit by the YRZ Green’s function, show that the FS and associated properties of high- T_c cuprate superconductors need not rely on the existence of exotic phenomena such as disconnected Fermi “arcs” for quantitative explanation.

The photoemission studies reported in this paper were carried out on underdoped cuprate samples, both Ca doped and oxygen deficient. The Ca-rich crystal was grown from a rod with $\text{Bi}_{2.1}\text{Sr}_{1.4}\text{Ca}_{1.5}\text{Cu}_2\text{O}_{8+\delta}$ composition using an arc-image furnace with a flowing 20% O_2/Ar gas mixture. The maximum T_c was 80 K. The sample was then annealed at 700 °C giving a 45 K T_c with a transition width of 2 K. The oxygen deficient $\text{Bi}_2\text{Sr}_2\text{CaCu}_2\text{O}_{8+\delta}$ crystals were produced by annealing optimally-doped Bi-2212 crystals, at 450 °C to 650 °C for 3 ~ 15 days. The spectra shown in this paper were all recorded on beamline U13UB at the NSLS using a Scienta SES2002 electron spectrometer. Each spectrum was typically recorded for a period of five to six hours in the pulse-counting mode with an energy and angular resolution of 15 meV and 0.1° respectively.

Figure 1 (a-f) shows photoemission spectra obtained near the end of the measured “Fermi arc” for an underdoped Bi2212 ($T_c = 65$ K) sample. The spectra in Fig. 1 (g-l) are shown after analysis using the Lucy-Richardson

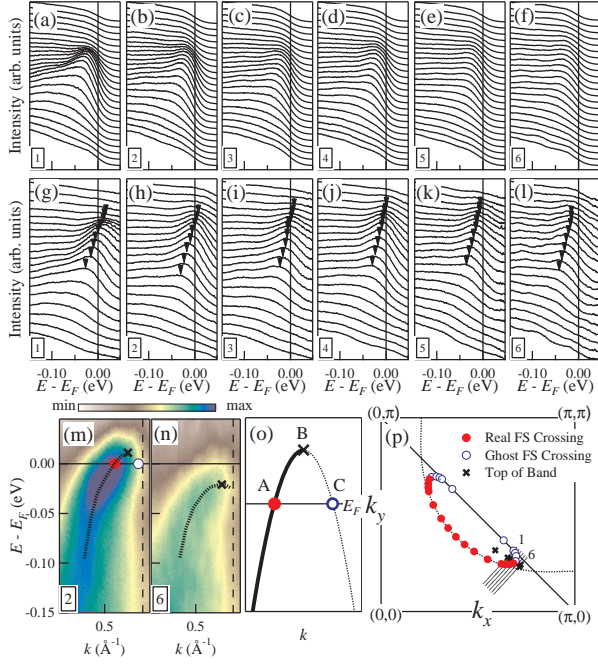


FIG. 1. Fermi surface of under-doped Bi2212 at 140 K ($T_c = 65$ K). (a-f) EDCs of raw data taken at cuts 1-6 in (p), and (g-h) after the analysis described in the text. The EDC peak positions are marked with triangles. In cuts 1-6, the band is slowly moving down with respect to E_F . Fermi surface crossing points exist in cuts 1-4, but not in cuts 5 & 6. These cuts demonstrate how the band sinks below E_F at the edge of the Fermi ‘‘pocket’’. (m) Image plot of cut 2 after Fermi normalization, with the FS crossing (red circle) and the top of the band (black cross) indicated. The ‘‘ghost’’ FS crossing (blue open circle) deduced from symmetrization in momentum is also indicated. (n) The same image plot for cut 6 showing no FS crossing. (o) Schematic showing points analyzed in the measured spectra as indicated in the text. (p) Pseudo-pocket determined for the 65 K sample. Red circles indicate the measured FS crossings corresponding to point A in the schematic. Crosses show the measured extremity of the dispersion corresponding to point B, and the open circles represent the ‘‘ghost’’ FS corresponding to point C. The dashed line indicates the large LDA FS.

(LR) deconvolution approach [16] to reduce the effects of the experimental resolution and after division by the appropriate temperature dependent Fermi function. This approach allows a more accurate determination of the FS crossings. The spectrum in Fig. 1(m) contains two experimental observations as indicated in the schematic in Fig. 1(o), the directly measured FS crossing, point A, and the point at which the dispersion comes to an abrupt halt, point B. We associate the point B with a gap in the spectral function reflecting the scattering of the photohole in the underlying spin liquid. As noted earlier, several calculations indicate that the formation of a Fermi hole pocket reflecting a particle-hole asymmetry in binding energy is derived from this scattering [5, 6]. Al-

ternative models that recognize the strong correlations in the system can also produce pockets [7, 17]. Within the YRZ ansatz, the pocket is formed by two band crossings, points A and C in the schematic, symmetric about the zone point associated with the bottom of the gap derived from the scattering, point B. Thus if we observe one FS crossing, point A, and the bottom of the gap, point B, we can in principle determine the other side of the pocket, the ‘‘ghost’’ FS, point C, as indicated in Fig. 1(p). The Fermi pocket derived in this manner is compared in the figure with the full FS traditionally assumed in ARPES studies. The deviation between latter FS and that determined in the present study becomes most evident near the end of the ‘‘arc’’. It is important to note that the hole pocket determined in this manner is clearly asymmetric with respect to the magnetic zone boundary, ruling out any pockets generated by scattering mechanisms simply associated with a $Q(\pi, \pi)$ vector. The ‘‘ghost’’ portion of the FS is, however, consistent with models showing a surface of zeros in the Green’s function at the chemical potential running along the magnetic zone boundary, defined by the line from $(0, \pi)$ to $(\pi, 0)$ [6, 18]. Under the condition, $G(\vec{k}, \omega) = 0$, the spectral weight measurable by photoemission is vanishingly small because the spectral function is defined by $A(\vec{k}, \omega) = -\text{Im}G(\vec{k}, \omega)$.

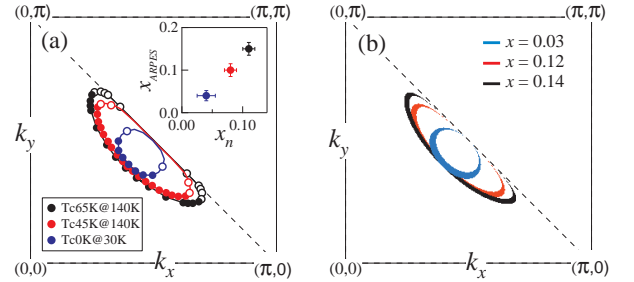


FIG. 2. (a) The pseudo-pockets determined for three different doping levels. The black data corresponds to the $T_c = 65$ K sample, the blue data corresponds to the $T_c = 45$ K sample and the red data corresponds to the non-superconducting $T_c = 0$ K sample. The area of the ‘‘pockets’’ x_{ARPES} scales with the nominal of doping level x_n , as shown in the inset. (b) The Fermi pockets derived from YRZ ansatz with different doping level.

Having determined the approximate shape and size of the pocket we can calculate the associated hole density for a given sample. Assuming the area inside the magnetic zone boundary corresponds to one electron at half filling, the pocket area corresponds to a hole carrier density of 0.15, higher than the doping level determined from the measured T_c alone. However the measured area is in reasonably good agreement with the area bounded by the locus of superconducting Bogoliubov band minima $k_B(E)$ extracted from SI-STs studies of a BSSCO sample with a similar doping level [19]. As such the combination of the two experiments raises obvious questions.

Does the pocket area really scale with the doping level and how is that consistent with earlier studies suggesting the “arc” length is temperature dependent with a length proportional to T/T^* [20] (Here T^* represents the doping dependent pseudogap temperature scale.) In attempting to answer these questions we show in Figure 2(a) a comparison of the FSs obtained using the present approach for the 65 K sample, a Ca doped sample ($T_c = 45$ K) and an oxygen-deficient non-superconducting sample ($T_c = 0$ K). It is clear from Fig. 2(a) that reducing the doping level into the highly underdoped regime results in a more noticeable deviation from the “LDA” FS. Further, while the measured areas of the different pockets, 0.15 holes ($T_c = 65$ K) 0.13 holes ($T_c = 45$ K) and 0.04 holes ($T_c = 0$ K) are larger than the presumed doping levels, 0.11, 0.085 and < 0.05 respectively. It is clear that the pocket size scales in relationship to the doping level as predicted theoretically [6, 10]. The finding of a finite nodal FS rather than a “nodal” point at low T for the $T_c = 0$ K sample is at variance with recently reported findings under the same conditions [21]. The measured Fermi pockets are however in good agreement with those predicted by the YRZ ansatz. In Fig. 2(b) we show the spectral function calculated at E_F as a function of doping, where $A(\vec{k}, 0) = -(1/\pi)\text{Im}G^{YRZ}(\vec{k}, 0)$ and where

$$G^{YRZ}(\vec{k}, \omega) = \frac{gt}{\omega - \xi_0(\vec{k}) - \Delta_R^2/[\omega - \xi_0(\vec{k})]}, \quad (1)$$

with associated parameters taken from reference [6]. The shape and area of the FS measured in ARPES are remarkably well reproduced by this model with the doping level as the only adjustable parameter.

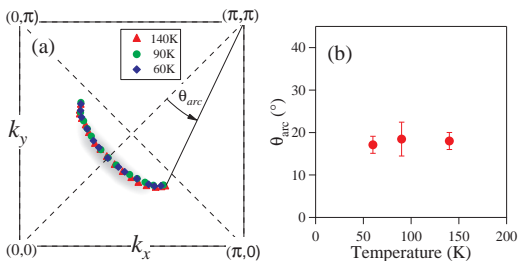


FIG. 3. (a) The Fermi surface crossings determined for the $T_c = 45$ K sample at three different temperatures. The triangles indicate measurements at a sample temperature of 140 K, the circles measurements at 90 K and the diamonds measurements at 60 K. (b) the measured arc lengths in (a) plotted as a function of temperature. We note that rather than cycling the temperatures on the same sample, the data in (a) are measured on different samples cut from the same crystal.

Turning to the question of whether the pocket areas are temperature dependent we show in Figure 3(a) the observed Fermi “arc” for the $T_c = 45$ K sample measured at three different temperatures: 60 K, 90 K and 140 K, all in the normal state but well below T^* . The measured FS crossings in the figure are determined by

the same method used in Figs. 1 and 2 rather than from the spectral weight at the Fermi level. In Fig. 3(b) we show the measured arc length as a function of temperature. It is clear that any change with temperature is minimal and certainly not consistent with an increase by more than a factor of two between the data taken at 140 K and 60 K as would be expected by a T/T^* scaling of the “arc” length [20]. This discrepancy arises because several experiments showing that the length of the Fermi “arc” scales as T/T^* depend upon an examination of the spectral weight at the chemical potential rather than the direct determination of whether or not a band actually crosses the chemical potential.

The picture of the low energy excitations of the normal state emerging from the present study is of a nodal FS characterized by a Fermi “pocket” that, at temperatures above T_c , shows a minimal temperature dependence and an area proportional only to the doping level. The bounds of this pocket are formed by smoothly connected surfaces of poles and zeros of the Green’s function well described by the YRZ ansatz. To fill out this picture of the normal state we turn our attention to the antinodal pseudogap itself.

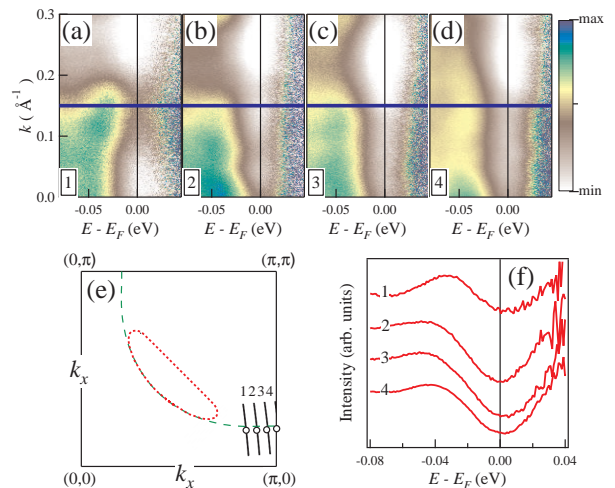


FIG. 4. (a-d) Spectra intensity measured at four points in the anti-nodal region as indicated in the schematic (e). The measurements are made with the sample in the normal state at a temperature of 140 K. (f) Intensity cuts through the spectral intensity maps of panel (a-d) as indicated by the lines in panel (a-d). They are also indicated by the open circles in (e).

Several theories of the pseudogap phase propose the formation of preformed singlet pairs above T_c in the anti-nodal region of the Brillouin zone [22]. The YRZ spin liquid based on the RVB picture is one such model as it recognizes the formation of resonating pairs of spin singlets along the copper-oxygen bonds of the square lattice as the lowest energy configuration. Fig. 4(a-d) shows a series of spectral plots along the straight sector of the

“LDA” FS in the anti-nodal region at a temperature of 140 K for the $T_c = 65$ K sample at the locations indicated in Fig. 4(e). Fig. 4(f) shows intensity cuts through these plots along the horizontal lines indicated in Fig. 4(a-d). It is evident that a symmetric gap exists at all points along this line. The particle-hole symmetry in binding energy observed here is in marked contrast to the particle-hole symmetry breaking predicted in the presence of density wave order and is a necessary condition for the formation of Cooper pairs. Thus the present observations add support to the hypothesis that the normal state is characterized by pair states forming along the copper-oxygen bonds and is consistent with earlier studies.

The combination of Fig. 2 and Fig. 4 points to a more complete picture of the low energy excitations in the normal state of the underdoped cuprates. For $T_c < T < T^*$, a Fermi “pocket” exists in the nodal region with an area proportional to the doping level. One does not need to invoke discontinuous Fermi “arc”s to describe the FS of underdoped Bi2212 and Luttinger’s sum rule, properly understood, is seen to still approximately stand. Although not verified in the present study one assumes that at some critical doping level greater than optimal, the reconstructed FS switches to the full Fermi surface as predicted in calculations [6, 10]. The full FS ought to also be visible for $T > T^*$, as has been observed recently in ARPES measurements [23]. In the underdoped regime, as one moves away from the pockets, two further distinct regions exist as manifested in the spectral intensity. The region in the immediate vicinity of the end of the pockets is characterized by a gap that is asymmetric with respect to the chemical potential. This gap again reflects the underlying spin correlation in the system. In the antinodal region, the gap becomes symmetric with respect to the chemical potential and is therefore indicative of incoherent preformed pairs of electrons in singlet states. This

picture of the FS appears to be entirely consistent with the momentum dependence of the gap function found in STS studies of the same material [24].

In conclusion, the photoemission measurements presented here show that the FS of the underdoped Bi2212 cuprate superconductors is defined not by disconnected “arcs”, but instead by fully closed hole pockets with areas proportional to the doping level and thus the carrier density of the system. The size and shape of these pockets are well reproduced within phenomenological models of the pseudogap state, such as the YRZ spin liquid, and are consistent with the doping in a Mott insulator. The absence of spectral weight on the “ghost” side of the pockets along the magnetic zone boundary results from the fact that quasiparticles in this region are defined by zeros, not poles, of the single particle Green’s function. These results show the cuprates evolve with doping from an antiferromagnetic insulator into a pseudogap state characterized by a heavily renormalized band structure and strong pairing correlations reflecting the underlying structure of the lattice. These are the essential characteristics of the underdoped cuprates, the unraveling of which is prerequisite to understanding the ultimate emergence of superconductivity below T_c .

The authors would like to thank Seamus Davis, Mike Norman, Maurice Rice, John Tranquada, Alexei Tsvelik, Subir Sachdev, Tonica Valla and Ali Yazdani for useful discussions. The work at Brookhaven is supported in part by the US DOE under Contract No. DE-AC02-98CH10886 and in part by the Center for Emergent Superconductivity, an Energy Frontier Research Center funded by the US DOE, Office of Basic Energy Sciences. The work at Argonne is partially supported by the Department of Energy under contract no. DE-AC02-06CH11357 and partially supported by the same Center for Emergent Superconductivity contract. T. E. Kidd acknowledges support from the Iowa Office of Energy Independence grant No. 09-IPF-11.

-
- [1] T. Timusk and B. Statt, Reports on Progress in Physics **62**, 61 (1999).
 [2] M. R. Norman *et al.*, Nature **392**, 157 (1998).
 [3] A. V. Chubukov and D. K. Morr, Physics Reports **288**, 355 (1997).
 [4] S. Chakravarty, C. Nayak, and S. Tewari, Phys. Rev. B **68**, 100504 (2003).
 [5] X. G. Wen and P. A. Lee, Phys. Rev. Lett. **80**, 2193 (1998).
 [6] K. Y. Yang, T. M. Rice, and F. C. Zhang, Phys. Rev. B **73**, 174501 (2006).
 [7] Y. Qi and S. Sachdev, Phys. Rev. B **81**, 115129 (2010).
 [8] P. W. Anderson, Science **235**, 1196 (1987).
 [9] K. Y. Yang *et al.*, Europhys. Lett. **86**, 37002 (2009).
 [10] J. P. F. LeBlanc, J. P. Carbotte, and E. J. Nicol, Phys. Rev. B **81**, 064504 (2010).
 [11] A. J. H. Borne, J. P. Carbotte, and E. J. Nicol, Phys. Rev. B **82**, 024521 (2010).
 [12] J. P. F. LeBlanc and J. P. Carbotte, arXiv:1006.5034.
 [13] R. M. Konik, T. M. Rice and A. M. Tsvelik, Phys. Rev. Lett. **96**, 086407 (2006).
 [14] H.-B. Yang *et al.*, Nature **456**, 77 (2008).
 [15] J. Meng *et al.*, Nature **462**, 335 (2009).
 [16] J. D. Rameau, H.-B. Yang, and P. D. Johnson, J. Electron Spectrosc. Relat. Phenom. **181**, 35 (2010).
 [17] M. Granath and B. M. Andersen, Phys. Rev. B **81**, 024501 (2010).
 [18] R. M. Konik, T. M. Rice, and A. M. Tsvelik, Phys. Rev. Lett. **96**, 086407 (2006).
 [19] Y. Kohsaka *et al.*, Nature **454**, 1072 (2008).
 [20] A. Kanigel *et al.*, Nature Phys. **2**, 447 (2006).
 [21] U. Chatterjee *et al.*, Nature Phys. **6**, 99 (2010).
 [22] V. J. Emery and S. A. Kivelson, Nature **374**, 434 (1995).
 [23] M. Hashimoto *et al.*, Nature Physics **6**, 414 (2010).
 [24] A. Pushp *et al.*, Science **324**, 1689 (2009).